

Optical absorption in GaTe under high pressure

J. Pellicer-Porres,* F. J. Manjón, A. Segura, and V. Muñoz

Institut de Ciència dels Materials Universitat de València, C/Doctor Moliner 50, E-46100 Burjassot (València), Spain

C. Power and J. Gonzalez

Centro de Estudio de Semiconductor (Universidad de los Andes), La Hechicera, Mérida 5251, Venezuela

(Received 22 April 1999)

This paper reports on the pressure dependence at room temperature of the absorption coefficient of the layered semiconductor gallium telluride. The absorption edge in the explored pressure range (up to 6.1 GPa) can be accounted for through the superposition and interaction of a direct gap and an indirect gap. The pressure shift of the direct gap is strongly nonlinear, starting at low pressure with a coefficient of -85.7 ± 0.4 meV/GPa and exhibiting a minimum at around 2.9 GPa. The exciton binding energy decreases under pressure, which can be related to the increase of the dielectric constant. The broadening of the exciton line is explained through phonon-assisted intervalley scattering of conduction-band electrons after the crossover between direct and indirect gaps, with an estimation of the related intervalley deformation potential.

[S0163-1829(99)16035-1]

I. INTRODUCTION

The layered materials of the III-VI family like gallium telluride or gallium selenide are of special interest for its potential applications in nonlinear and optical bistable devices.^{1,2} GaTe is a direct-gap semiconductor³⁻⁶ with strong excitonic absorption at room temperature (RT). GaTe belongs to the space group⁷ $B2/m$, which has a monoclinic unit cell. The layer structure of GaTe, as like that of GaSe, is composed of a four-sheet Te(Se)-Ga-Ga-Te(Se) intralayer stacking pattern in which the bonds are mainly covalent with some ionic contribution, while interlayer bonds are of weak van der Waals type. But, in contrast to GaSe, one-third of the Ga-Ga bonds lies almost in the layer plane. Band-structure calculations are not available at present, because of the complexity of the crystallographic unit cell, that contains 12 molecules (108 valence electrons). This explains why GaTe is one of the less-studied III-VI layered semiconductors. The study under pressure allows one to tune the degree of anisotropy in bonding, and helps to understand the nature of interactions. The pressure effects in related materials like GaSe (Ref. 8) and InSe (Ref. 9) have been studied in recent years but, to the best of our knowledge, only Niilisk¹⁰ studied the low-pressure energy shift of the band gap in GaTe through photoconductivity experiments, whose intrinsic accuracy is not as good as the one obtained by optical measurements, as photoconductivity spectra depend on the carrier diffusion length and surface recombination velocity.

X-ray-diffraction (XRD) and optical reflectivity measurements¹¹ report on the pressure dependence of GaTe lattice parameters up to 8 GPa, and show that this material undergoes a first-order transition at 10 GPa into a new metallic high pressure polymorph with NaCl-type structure, similar to that observed in InSe at 10 GPa. In addition, recent x-ray-absorption spectroscopy (XAS) experiments¹² report on the pressure dependence of the Ga-Te and Ga-Ga bond lengths.

In this work we present measurements of the absorption

edge under pressure at RT. Experimental details are given in Sec. II. Section III is devoted to the presentation, interpretation and discussion of the experimental results. Finally, conclusions are presented in Sec. IV.

II. EXPERIMENT

The GaTe single crystals used in this work were cleaved from an ingot grown by the Bridgman-Stockbarger method. The samples were easily cleaved in the layer plane due to the existence of weak interlayer bonds. They were prepared with dimensions $100 \times 100 \times 6.1$ and $100 \times 100 \times 4.6 \mu\text{m}^3$, and with the larger faces parallel to the layer plane. In each case the sample was placed just after the cleavage together with a ruby chip in a 200- μm -diameter hole drilled on a 60- μm -thick Inconel gasket and inserted between the diamonds of a diamond-anvil cell (DAC).¹³ A 4:1 methanol-ethanol mixture was used as pressure transmitting medium to ensure hydrostatic conditions^{13,14} up to 10 GPa. The pressure was measured from the shift of the R_1 line of the ruby fluorescence. Two experimental arrangements were utilised. With the 6.1- μm sample, we used a membrane DAC (MDAC).¹⁵ In this case, the optical source was a tungsten lamp chopped at 180 KHz. The light from the lamp was collimated and focused on the MDAC as a 40- μm spot. The transmitted light was newly collimated, spatially filtered and focused on the entrance slit of a Jovin-Ivon THR 1000 monochromator, with a dispersion of 16 Å/mm in the slit plane. The photodetector was a Si photodiode whose signal was synchronously measured with a lock-in amplifier. In the case of the 4.6- μm sample, we used a Piermarini and Block cell.¹⁶ In this setup we utilized a 1681 SPEX spectrometer with a grating of 1200 grooves/mm and a focal of 0.22 m. The light exiting the monochromator was detected with a photomultiplier. All measurements were performed at RT, with incident nonpolarized light propagating in the direction perpendicular to the layers.

The transmittance was measured in the DAC up to 12

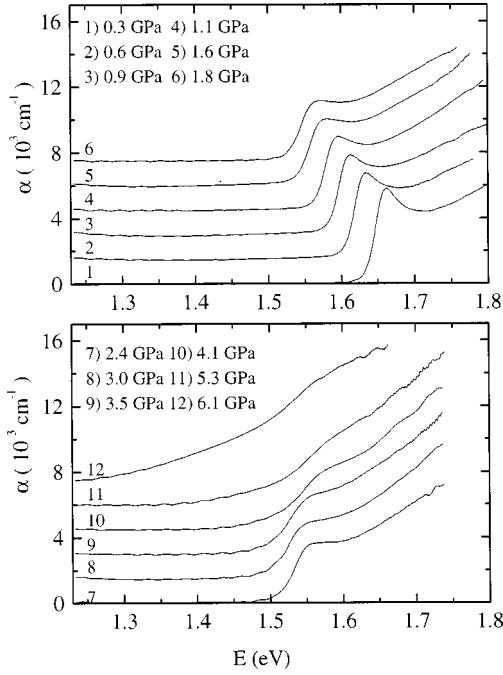


FIG. 1. Pressure evolution of the experimental absorption coefficient for GaTe in the direction perpendicular to the layers ($T = 300$ K). The curves are shifted 1500 cm^{-1} for clarity.

GPa using the sample-in sample-out method.⁸ Although stray light was minimized by spatial filtering, we measured residual stray light in the high absorption region of the sample. The contribution to the spectrum coming from the residual stray light was removed by subtracting the minimum transmittance to every experimental spectrum. Then a correction was made to obtain the theoretical transmittance by adjusting the experimental transmittance at the spectral range where the sample is transparent to the theoretical value. This range is fixed using the criterion of constant transmittance. With the increase of light scattering at high pressure, this criterion becomes very loose, and we limited the analysis to spectra taken up to 6.1 GPa. Finally, the absorption coefficient α was calculated taking into account the theoretical transmittance, the thickness of the sample and its reflectivity, which is a function of the refractive indexes of GaTe and that of the ethanol-methanol mixture (given under pressure as a function of frequency in Ref. 17). The sample thickness at ambient pressure was determined from the interference fringe pattern in the transparent region. Its variation with pressure was calculated from the compressibility given in Ref. 11.

We should point out that we observed transmitted light up to 9.4 GPa, with a higher presence of scattered light as pressure increased. Above this pressure the sample became opaque. This result agrees with the transition, at 10 GPa, to a high pressure polymorph of the NaCl structure described in Ref. 11.

III. RESULTS AND DISCUSSION

A. Optical absorption coefficient as a function of pressure

In Fig. 1 we present the evolution of the absorption edge of GaTe at RT from ambient pressure up to 6.1 GPa. The exciton structure is clearly observable up to 1.8 GPa. Above

2.4 GPa a low-energy tail appears. As in GaSe, this is associated with the red shift of the indirect absorption edge.

Following Elliot,¹⁸ the optical absorption is enhanced by the interaction between the electron and the hole. According to Toyozawa,¹⁹ when the electron lattice coupling is strong or the temperature is high, the line shapes of the exciton are Gaussian. Thus, in the Elliot-Toyozawa model, the absorption is given by

$$\alpha(E) = \frac{C_0 R^{1/2}}{E} \left\{ \sum_{m=1}^{\infty} \frac{2R}{m^3} \frac{1}{\Gamma_m \sqrt{2\pi}} e^{-(E-E_m)^2/2\Gamma_m^2} + \int_{E_0}^{\infty} dE' \frac{1}{1 - e^{-2\pi\sqrt{R/E'-E_0}}} \frac{1}{\Gamma \sqrt{2\pi}} e^{(E'-E)^2/2\Gamma_c^2} \right\}, \quad (1)$$

with

$$C_0 = \frac{4\pi^2 (2\mu)^{3/2} e^2 |M_R|^2}{nc\hbar^2 m_0^2}, \quad (2)$$

$$E_m = E_0 - R/m^2. \quad (3)$$

Here R is the Rydberg energy, E_0 the gap, μ the exciton reduced mass, m_0 the free-electron mass, n the refractive index, M_R the matrix element for electron-photon interaction, Γ_c the continuum width, and E_m and Γ_m the energy and half-width of the m th exciton line respectively. For the half-width of the m th line we used the empirical relation²¹

$$\Gamma_m = \Gamma_e - (\Gamma_e - \Gamma_1)/m^2, \quad (4)$$

In order to obtain an analytical expression to be used in a least-square fitting procedure, we approximated the contribution of the continuum in the Elliot's formula [Eq. (1)] by a Heaviside function. In this way we obtained

$$\alpha(E) = \frac{C_0 R^{1/2}}{E} \left\{ \sum_{m=1}^{\infty} \frac{2R}{m^3} \frac{1}{\Gamma_m \sqrt{2\pi}} e^{-(E-E_m)^2/2\Gamma_m^2} + \frac{1}{2} \left[1 - \text{Erf} \left(\frac{E_0 - E}{\sqrt{2}\Gamma_c} \right) \right] \right\}. \quad (5)$$

For $E < E_0 + 2R$ the approximation leads to a relative error smaller than 1%, and for $E < E_0 + 4R$ smaller than 5%.

The shape of the exciton peak at RT is clearly asymmetric. Attempts to fit the peak with asymmetric function shapes lead to extra parameters with no physical meaning. Nevertheless, from the study of GaTe at low temperature,³ we know that the main part of this asymmetry is due to the presence of a very intense peak at about 17 meV above the exciton. This energy corresponds to that of one strong feature in infrared absorption and reflection spectra corresponding to resonant absorption of a 18-meV polar-optical phonon.²⁰ A similar peak is also observed in the absorption edges of GaSe (Ref. 21) and InSe,²² and has been attributed to a resonant absorption with creation of excitons and LO polar phonons. In GaSe and InSe this peak is relatively weak, and can be neglected in the fitting procedure. On the conversely its integrated intensity in GaTe is comparable to

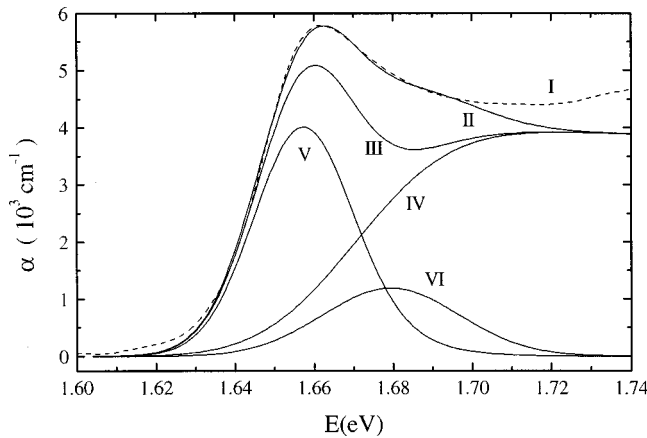


FIG. 2. Experimental and fitted optical absorption spectrum for GaTe at $P=0.3$ GPa. The curve labeled *I* represents the experimental spectrum, curve *II* the theoretical fit, curve *III* the theoretical fit without the optical phonon contribution, curve *IV* the continuous part, curve *V* the discrete one, and curve *VI* the optical-phonon contribution.

that of the exciton and does not decrease in the temperature range through which it does not overlap with the exciton.³ It is reasonable to assume that it is also present at RT, and contributes to the asymmetry of the observed peak. In order to introduce this contribution we limit ourselves to describing it in a phenomenological way. An analysis of its variation on temperature showed that its energy position respect to the exciton remains constant from 30 to 190 K. As concerns its temperature broadening, it can be reproduced by convolution of its low-temperature shape with the excitonic peak at a given temperature. Then we assume that its behavior under pressure can be obtained in the same way. The ratio between the intensity of the exciton absorption and the one coming from the creation of an exciton with simultaneous emission of a LO phonon is maintained constant for different pressures in the fitting procedure. The pressure dependence of phonon frequencies in GaTe has not been measured. By comparison with related compounds InSe and GaSe, an increase of the order of 6% is expected in the explored pressure range. Then this variation can be neglected in this analysis.

In Fig. 2 we show, as an example, the analysis of the spectrum taken at 0.3 GPa. All the contributions are detailed: curve *I* represents the experimental spectrum, curve *II* the theoretical fit, curve *III* the theoretical fit without the optical-phonon contribution, curve *IV* the continuous part, curve *V* the discrete part and, finally, curve *VI* the optical phonon contribution.

The indirect absorption contribution which becomes apparent at 2.4 GPa was described through the usual equation for an indirect edge,²³ neglecting the contribution of absorption of a phonon because it is representative only in the low absorption tail, that could not be measured with such a thin sample. In this way we were able to deduce the pressure shift of the energy of the indirect edge plus the energy of the phonon that takes part in the process. In the high-pressure spectra the indirect edge is clearly separated, and its pressure coefficient can be determined. Below 1.5 GPa its contribution is too weak and the fitting procedure yields very large uncertainties for the indirect edge parameters.

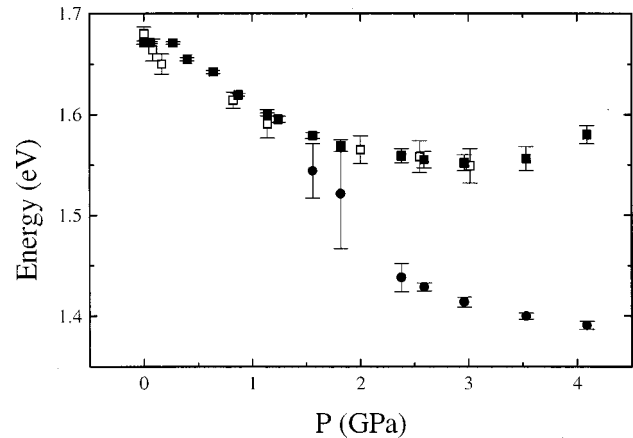


FIG. 3. Variation of direct and indirect gaps under pressure. The squares and circles represent values of the direct and indirect gaps, respectively. Filled symbols: 6.1- μm sample. Hollow symbols: 4.6- μm sample.

B. Pressure dependence of direct- and indirect-band-gap energies

Figure 3 gives the pressure dependence of both direct and indirect gaps. As in GaSe and InSe, the pressure dependence of the direct gap is strongly nonlinear, with a minimum that occurs at a much higher pressure, 2.9 GPa (P_m), with respect to InSe ($P_m=0.5$ GPa) or GaSe ($P_m=1.3$ GPa). The band gap at room pressure is 1.680 ± 0.004 eV, in accordance with previous results.³⁻⁶ At low pressure the direct gap shifts at a rate 85.7 ± 0.4 meV/GPa, a larger absolute value than those of InSe and GaSe, which are about -17 and -45 meV/GPa, respectively. Our result is also to be compared with the one obtained in Ref. 10 for GaTe, -100 meV/GPa. The slight disagreement can be accounted for by the fact that the photoconductivity edge depends not only on the band gap, but also on magnitudes such as the carrier diffusion length or surface recombination velocity, whose pressure dependence is not known.

In the pressure range where the GaTe indirect gap can be determined, its behavior is similar to that of GaSe and InSe,^{8,24} with a pressure coefficient that decreases with increasing pressure. Adjusting its dependence to a second-order equation, we can obtain a rough approximation of its value at room pressure (1.82 eV) and the direct to indirect crossover pressure (1.2 GPa).

The band structure of GaTe is not known. The band structures of InSe and GaSe could be a good starting point for any band-structure consideration in GaTe, based on the fact that, in spite of the crystal structure differences, the three compounds share the same kind of intralayer and interlayer bonds and atomic coordination. The main novelty is that one-third of the Ga-Ga bonds lies almost in the layer plane. Because of this, in the direction perpendicular to the c axis, the fundamental translation in the layer plane includes three units Ga_2Te_2 (and not one as in the other compounds). The main features of band structure could be deduced through a triple folding of InSe band structure in one direction of the layer plane, as in both compounds all layers are equivalent. This folding should not change the character of the upper valence and lower conduction bands.

In order to explain the pressure variation of the band gap in III-VI layered semiconductors a simple model was developed in previous works,^{8,9} based on the assumption that the layer compressibility is isotropic. In this model, the topmost valence band and the lowest conduction band originate mainly from sp_z orbitals (cation s orbitals and anion p_z orbitals), showing in the first place a strong bonding-antibonding repulsion attributed to the covalent character of the intralayer bonding, and, second, by a band widening caused by the interaction of p_z orbitals. Consistently, the band-gap variation was written in terms of intralayer and interlayer distances, and deformation potentials for both distances were deduced. On the same hypothesis, one can calculate intralayer and interlayer compressibilities from XRD experiments under pressure,⁸ and deduce the deformation potentials in GaTe by fitting to experimental results of Fig. 3. The deformation potentials turn out to be $dE/dc_i = -2.4 \pm 0.5$ eV/Å for the intralayer distances, and $dE/dc_l = -1.1 \pm 0.2$ eV/Å for the interlayer distances. Coherently with the higher pressure for the gap minimum, the interlayer potential in GaTe is higher than in GaSe and InSe.

However, recent XAS experiments^{12,25,26} show that in GaTe, GaSe, and InSe, pressure originates structural changes inside the layers that cannot be described by a simple compressibility parameter. This effect consists in a considerable augmentation of the angle between the anion-cation bond and the anion planes, which introduces a positive contribution to the anion-anion intralayer distance that is not compensated for by the bond-length decrease. Consequently, the layer thickness that was used in previous models increases with pressure. The application of the above mentioned simple models would lead to deformation potentials with no physical meaning. As a result, it is necessary the use of a more sophisticated model for the band-gap variation, based on pseudopotential or linear muffin-tin orbital methods,^{27,28} recently applied to the investigation of band structure in InSe. Under a slightly different point of view, in these models the upper valence band would come mainly from anion nonbonding p_z states, and the lower conduction band from antibonding cation s states, with a certain mixture of cation and anion p_z orbitals. The most important contribution to the linear positive shift of the conduction band can be attributed to the increase of bonding-antibonding splitting of the cation s level caused by the cation-cation bond-length decrease. The positive nonlinear shift of the valence band can be attributed in its turn to the increase of overlap between anion p_z orbitals of adjacent layers. The nonlinearity is attributed to the strong interaction between the anions in the interlayer space. At low pressure this term dominates as the interlayer distances decrease very quickly, which results in a negative pressure coefficient for the band gap. The variation of the interlayer distance is strongly nonlinear and tends to saturate. Then, at higher pressures, the cation bonding-antibonding splitting dominates and the pressure coefficient of the band gap becomes positive. From the tilt of the Te P_z orbitals with respect to the layer planes and the larger extent of these orbitals (with respect to the Se p_z orbitals) a stronger interlayer interaction could be expected. As the interlayer interaction is stronger the interaction between the p_z orbitals of tellurium is more effective, and the minimum bandgap is reached at a higher pressure. Attempts to describe results of

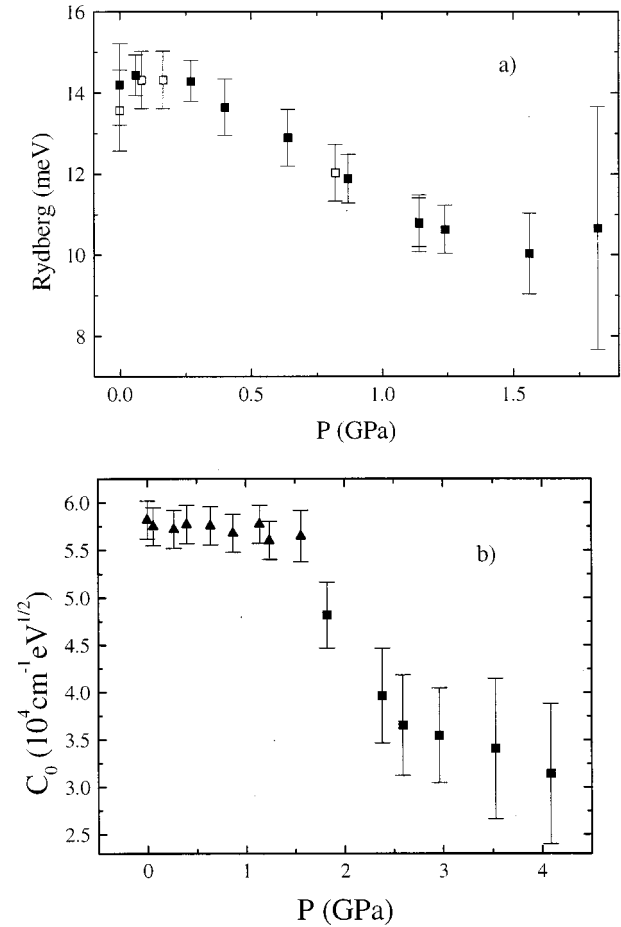


FIG. 4. (a) Variation of the exciton binding energy as a function of pressure. Filled symbols: 6.1- μm sample. Hollow symbols: 4.6- μm sample (b) Evolution under pressure of C_0 [see Eq. (2) for definition]. Triangles: Fit carried out taking into account only of the direct edge contribution. Squares: Fit carried out including both the direct and indirect edges.

Fig. 3 with deformation potentials for the cation-cation bond length and the average anion-anion intralayer distance (as deduced from XAS experiments) have failed. This failure is understandable when one takes into account that the relative change of the interlayer distance from ambient pressure to 3 GPa is as large as 30%. On the other side hand, the bond-angle variation strongly affects the orbital mixing in each band and limits the validity of simple deformation potential models. Full band structure calculations seem to be necessary to explain these results.

C. Exciton Rydberg variation under pressure

The pressure dependence of the exciton Rydberg as obtained from our fitting procedure is shown in Fig. 4(a). At ambient pressure the value found was 14.2 ± 1.0 meV. Previous works^{3,29} reported values of the order of 16 meV at 30 K, which are coherent with ours if we take into account the expected increase in the dielectric constant and decrease of the effective masses when increasing the temperature up to RT. The static dielectric constant can be estimated from the electronic contribution³ and the LO and TO frequencies³⁰ through the Lyddane-Sachs-Teller relation, yielding $\epsilon_0 = 12.5$. Due to the lack of information about the dielectric

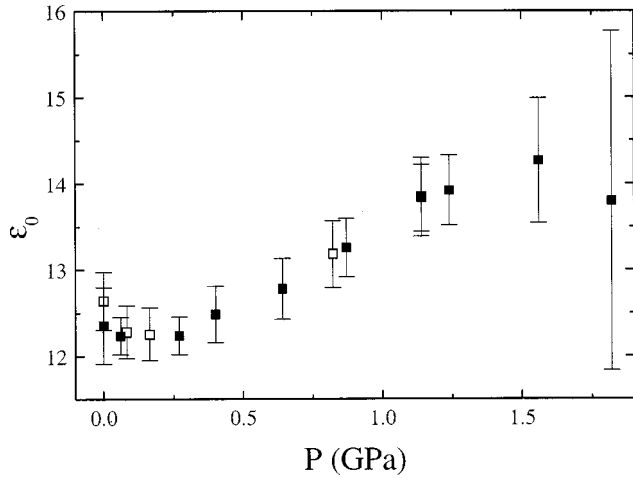


FIG. 5. Calculated variation of the static dielectric constant. Filled symbols: 6.1- μm sample. Hollow symbols: 4.6- μm sample.

constant and effective-mass anisotropy, we will discuss the results on the basis of an isotropic model,

$$R = R_{\infty} \frac{\mu}{\epsilon_0}, \quad (6)$$

where R_{∞} is the hydrogenic Rydberg, μ is the effective exciton mass, and ϵ_0 the static dielectric constant. At ambient pressure, Eq. (6) yields $\mu = 0.14m_0$.

According to the $\mathbf{k} \cdot \mathbf{p}$ model, if the matrix element of the fundamental transition is high enough to dominate with respect to higher-energy transitions, the electron effective mass is proportional to the direct gap. As the absorption coefficient at the gap is half the typical values for III-V semiconductors like GaAs, one can assume that the $\mathbf{k} \cdot \mathbf{p}$ model applies reasonably well. As the hole effective mass in III-VI chalcogenides is very high, we can assume that the exciton reduced mass is very close to the electron effective mass. With these assumptions, the pressure dependence of the static dielectric constant can be calculated from the pressure dependence of the exciton Rydberg, as shown in Fig. 5. At ambient pressure the pressure coefficient is $d\epsilon_0/dP \approx 1.3 \text{ GPa}^{-1}$. From refractive index measurements under pressure it is known that the increase of the electronic contribution for polarization parallel to the layers is of the order of $d\epsilon_{\infty}/dP \approx 0.33 \text{ GPa}^{-1}$. We can conclude that GaTe behaves as GaS, GaSe, and InSe, and exhibits a strong increase under pressure of the static dielectric constant for polarization perpendicular to the layers. It has been recently shown that this increase is mainly of electronic origin.³¹ The contribution of Van der Waals forces to crystal binding along that direction would make layered semiconductors to behave as molecular solids^{31,32} for polarization perpendicular to the layers. Band broadening effects dominate the pressure dependence of the effective Penn gap, which decreases under pressure, leading to the strong increase of the electronic polarizability.

D. Evolution of the matrix element with pressure

Figure 4(b) shows the evolution of the C_0 constant under pressure. A clear decrease is observed in the whole pressure

range. The less pronounced decrease in the low-pressure range can be attributed to the fact that the indirect-gap contribution was not included in the fitting procedure, in order to reduce the number of fitting parameters. Also, from 1 GPa on, the exciton structure begins to smear and it is difficult to separate the contributions from C_0 and the exciton Rydberg to the absorption intensity [Eq. (5)]. Consequently, the error in the determination of C_0 increases. The fact that the decrease of C_0 is larger than that expected from the $E_g^{3/2}$ dependence indicates a decrease of the matrix element under pressure, that has been already observed in GaSe.⁸ As the allowed character of the fundamental transition (for polarization parallel to the layers) is attributed to the contribution of lower valence bands with $p_x - p_y$ character to the uppermost valence band (mainly with p_z character), the decrease of the matrix element indicates that the band mixing decreases under pressure due to the increase of the energy difference (ΔE_{v12}) between those bands, that has been actually observed in GaSe.³³ In InSe, the matrix element also exhibits a behavior clearly correlated with this energy difference: it decreases in the low-pressure range (through which ΔE_{v12} increases) and increases above 2 GPa (when ΔE_{v12} decreases).³⁴ Results of Fig. 4(b) suggest that, in spite of the crystal structure differences, the behavior of the matrix element is also correlated with the energy difference ΔE_{v12} . As the direct band gap in GaTe exhibits a wider range with a negative pressure coefficient, one would also expect ΔE_{v12} to increase in a wider pressure range (with respect to GaSe and InSe). This energy difference would be not so strictly correlated with the spin-orbit splitting in the anion as proposed by several authors.^{6,35} In fact, attempts to apply Hopfield's quasicubic mode³⁶ to InSe and GaSe band structure²² are in contradiction with recent first-principles band structure calculations in InSe,²⁷ showing that the value of ΔE_{v12} in the Z point of the rhombohedral Brillouin zone (where the maximum of the uppermost valence band lies) is mainly due to the large dispersion of this band along the ΓZ direction. In the Γ point, where the Hopfield model should be applied, the order of the bands is reversed and the $p_x - p_y$ bands lie about 0.4 eV above the p_z band. If GaTe had an InSe structure, with the higher spin-orbit splitting in Te (about 1 eV), one could obtain its valence-band structure from the InSe band structure by shifting the p_z nonbonding band down in energy by about 0.6 eV [the difference in the spin-orbit splitting between Te and Se (Ref. 37)] with respect to the $p_x - p_y$ bands. If we assume the same width for the p_z band, ΔE_{v12} in the Z point would be about 0.5 eV (compared to 1.1 eV in InSe). If the band mixing is proportional to $(\Delta E_{v12})^{-1}$, the matrix element would be approximately four times that of InSe, as it actually occurs. Obviously, GaTe does not have an InSe rhombohedral structure, but, as was mentioned in Sec. III B, it also consists of one layer per unit cell and the anion distribution is very similar to that of InSe, which means that the dispersion of the nonbonding p_z upper valence band cannot be very different from that of InSe. The lower symmetry in the GaTe planes (with six molecules per unit cell) can be introduced by a triple folding in one direction of the layers, that should not affect the character and dispersion of the uppermost valence band. The existence of the in-plane Ga-Ga bonds distorts the disposition of the anions (that do not lie in a plane) and in-

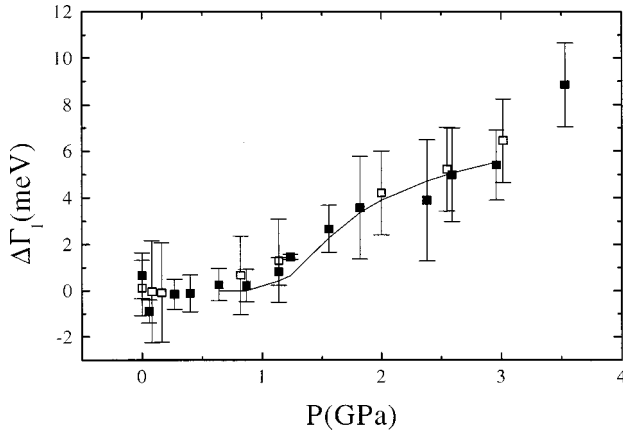


FIG. 6. Variation of the half-width Γ_1 of the $1s$ exciton line under pressure. Γ_1 is constant until the crossover ($P=1.2$ GPa). From this point on it increases due to intervalley scattering. Filled symbols: $6.1\text{-}\mu\text{m}$ sample. Hollow symbols: $4.6\text{-}\mu\text{m}$ sample.

creases the anion-anion interaction between the half layers. This should result also in a stronger mixing of the uppermost Te p_z nonbonding band with the lower Te p_x - p_y bands

E. Exciton broadening with pressure

Figure 6 shows the values of the half-width Γ_1 with pressure. Within the fit uncertainty Γ_1 is fairly constant up to 1.2 GPa and increases above this pressure. As this is the crossover pressure, the broadening can be attributed to intervalley scattering between the conduction-band minima corresponding to direct and indirect transitions.

From the line broadening effect we can estimate the corresponding phonon deformation potential. Within the effective-mass approximation the exciton broadening $\Delta\Gamma_1$ induced by scattering with zone-edge phonons can be expressed as a function of the energy difference between the conduction-band minima:³⁸

$$\Delta\Gamma = \frac{S}{E_q} [(N_q + 1)\Theta(\Delta E_{12} - E_q)\sqrt{\Delta E_{12} - E_q} + N_q\sqrt{\Delta E_{12} + E_q}], \quad (7)$$

with

$$S = \frac{Mm_2^{3/2}D_{12}^2}{2\sqrt{2}\pi\hbar\rho} \quad (8)$$

Here Θ is the Heaviside function, E_q and N_q are the energy and the occupation number of the phonon involved in

the scattering, ΔE_{12} is the energy difference between the indirect and direct gaps, $\rho=5.44\text{ g/cm}^3$ is the density for GaTe, m_{02} is the density-of-states effective mass at the second minimum point of the conduction band, D_{12} is the phonon deformation potential for intervalley phonon scattering, and M is the number of equivalent indirect minima in the conduction band.

Unfortunately, very little is known about the structure of the conduction band in GaTe nor the position of the excited minima in the first Brillouin zone. We can in any case show that Eq. (8) reproduces the observed pressure evolution. The symmetry of the monoclinic cell implies $M=2$ (if the minima are on the mirror plane or on the second-order rotation axis) or $M=4$ (if the minima are elsewhere). In the second hypothesis, and assuming a value $m_2=0.4m_0$ (as in InSe), fitting Eq. (7) to the experimental data yields $D_{12}=3.0\pm 1.5\text{ eV/\AA}$ and $E_q=21\pm 11\text{ meV}$.

IV. CONCLUSIONS

We have extended to GaTe the optical studies that have been carried out in other layered semiconductors of the same family, like GaSe or InSe. As concerns the optical absorption analysis, the main difference with these compounds has been the necessity of including the contribution of resonant absorption with creation of excitons and LO polar phonons. The behavior of the gap under pressure is highly nonlinear, showing a minimum at 2.9 GPa, a higher value than the one obtained for GaSe and InSe. The reason for this difference is that although the intralayer interaction is of the same nature as that in InSe or GaSe, the interlayer interaction is clearly stronger, due to the tilt of Te p_z orbitals and the larger extent of these orbitals with respect to Se. The pressure dependence of the Rydberg energy is mainly accounted for by the large increase of the dielectric constant. The observed decrease of the direct transition matrix element seems to be correlated with the increase of the energy difference between the p_z antibonding uppermost valence band and lower valence bands with p_x and p_y character. We also shared the decrease of the indirect gap under pressure. The crossover results at 1.2 GPa, were shown both by the pressure dependence of the gaps and by the sudden increase in the exciton width, this last one explained through the intervalley scattering between conduction-band minima.

ACKNOWLEDGMENTS

This work was supported by the Spanish government CICYT under Grant No. MAT95-0391 and by Generalitat Valenciana under Grant No. D.O.G.V. 2784.

*Author to whom correspondence should be addressed. FAX: (34) 6-3983146. Electronic address: Julio.Pellicer@uv.es

¹W. C. Eckhoff, R. S. Putnam, S. Wang, R. F. Curl, and F. K. Tittel, *Appl. Phys. B: Solids Surf.* **63**, 437 (1996).

²M. A. Hernández, J. F. Sánchez, M. V. Andrés, A. Segura, and V. Muñoz, *Óptica Pura y Aplicada* **26**, 152 (1993).

³J. F. Sánchez-Royo, A. Segura, and V. Muñoz, *Phys. Status Solidi A* **151**, 257 (1995).

⁴A. Gousskov, J. Camassel, and L. Gousskov, *Prog. Cryst. Growth Charact.* **5**, 323 (1982).

⁵J. Camassel, P. Merle, and H. Mathieu, *Physica B & C* **99**, 309 (1980).

- ⁶J. Camassel, P. Merle, H. Mathieu, and A. Gouksov, *Phys. Rev. B* **19**, 1060 (1979).
- ⁷M. Julien-Pouzol, S. Jaulmes, M. Guittard, and F. Alapini, *Acta Crystallogr. B* **35**, 2848 (1979).
- ⁸M. Gauthier, A. Polian, J. M. Besson, and A. Chevy, *Phys. Rev. B* **40**, 3837 (1989).
- ⁹A. R. Goñi, A. Cantarero, U. Schwarz, K. Syassen, and A. Chevy, *Phys. Rev. B* **45**, 4221 (1992).
- ¹⁰A. J. Niilisk and J. J. Kirs, *Phys. Status Solidi* **31**, K97 (1969).
- ¹¹U. Schwarz, K. Syassen, and R. Knierp, *J. Alloys Compd.* **224**, 212 (1995).
- ¹²J. Pellicer-Porres, A. Segura, A. San Miguel, and V. Muñoz, *Phys. Status Solidi B* **211**, 389 (1999).
- ¹³M. Eremets, *High Pressure Experimental Methods* (Oxford University Press, Oxford 1996).
- ¹⁴G. J. Piermarini, S. Block, and J. S. Barnett, *J. Appl. Phys.* **44**, 5377 (1973).
- ¹⁵R. Le Toullec, J. P. Pinceaux, and P. Loubeyre, *High Press. Res.* **1**, 77 (1988).
- ¹⁶G. J. Piermarini and S. Block, *Rev. Sci. Instrum.* **46**, 973 (1975).
- ¹⁷J. H. Eggert, L. Xu, R. Che, L. Chen, and J. Wang, *J. Appl. Phys.* **72**, 2453 (1992).
- ¹⁸R. J. Elliot, *Phys. Rev.* **108**, 1384 (1957).
- ¹⁹Y. Toyozawa, *Prog. Theor. Phys.* **20**, 53 (1958).
- ²⁰J. C. Irwin and B. P. Clayman, *Phys. Rev. B* **19**, 2099 (1978).
- ²¹R. Le Toullec, N. Piccioli, and J. C. Chervin, *Phys. Rev. B* **22**, 6162 (1980).
- ²²N. Kuroda, I. Munakata, and Y. Nishina, *Solid State Commun.* **33**, 687 (1980).
- ²³O. Madelung, *Introduction to Solid State Theory* (Springer-Verlag, Berlin 1981).
- ²⁴D. Errandonea, F. Manjón, J. Pellicer-Porres, A. Segura, and V. Muñoz, *Phys. Status Solidi B* **211**, 33 (1999).
- ²⁵J. Pellicer-Porres, A. Segura, V. Muñoz, and A. San Miguel (unpublished).
- ²⁶J. P. Itié, A. Polian, M. Gauthier, and A. San Miguel (unpublished).
- ²⁷Gomes da Costa, R. G. Dandrea, R. F. Wallis, and M. Balkanski, *Phys. Rev. B* **48**, 14 135 (1993).
- ²⁸C. Ulrich, A. R. Goñi, K. Syassen, O. Jepsen, A. Cantarero, and V. Muñoz, in *Proceedings of the Joint XV AIRPAT and XXXIII EHPRG International Conference, 1995* (World Scientific, Singapore, 1996); C. Ulrich, Ph.D. thesis, Universität Stuttgart, 1997.
- ²⁹J. Z. Wan, J. L. Brebner, R. Leonelli, G. Zhao, and J. T. Graham, *Phys. Rev. B* **46**, 1468 (1993).
- ³⁰G. L. Belenkii, L. N. Alieva, R. K. H. Nani, E. Yu. Salaev, and V. Ya. Shteinshraiber, *Fiz. Tverd. Tela (Leningrad)* **19** 282 (1977) [*Sov. Phys. Solid State* **19**, 162 (1977)].
- ³¹D. Errandonea, A. Segura, V. Muñoz, and A. Chevy, *Phys. Status Solidi B* **211**, 201 (1999).
- ³²R. A. Weinstein, R. Zallen, M. L. Slade, and A. de Lozanne, *Phys. Rev. B* **24**, 4652 (1981).
- ³³N. Kuroda, O. Ueno, and Y. Nishina, *J. Phys. Soc. Jpn.* **55**, 581 (1986).
- ³⁴F. J. Manjón, Ph.D. thesis, University of Valencia, 1999.
- ³⁵N. Kuroda, I. Munakata, and Y. Nishina, *Solid State Commun.* **33**, 687 (1980).
- ³⁶J. J. Holpfield, *J. Phys. Chem. Solids* **15**, 97 (1960).
- ³⁷D. J. Chadi, *Phys. Rev. B* **16**, 790 (1977).
- ³⁸A. R. Goñi, A. Cantarero, K. Syassen, and M. Cardona, *Phys. Rev. B* **41**, 10 111 (1990).